Supporting Information

Quantitative Insights into Non-Uniform Plasmonic Hotspots due to Symmetry Breaking Induced by Oblique Incidence

Yong Zhou[*#a], Hongliang Li[#c], Guanhua Zhang[#b], Dong Wei[b], Lan Zhang[c], Yujie Meng[a], Xianfeng Zheng[a], Zhibo Ma[*b], Jie Zeng[*c], and Xueming Yang[b,d]

[a]Anhui Key Laboratory of Optoelectric Materials Science and Technology, Department of Physics, Anhui Normal University, Wuhu, Anhui 241000, P. R. China. E-mail: yong.zhou@mail.ahnu.edu.cn

[b]State Key Laboratory of Molecular Reaction Dynamics, Dalian Institute of Chemical Physics, Chinese Academy of Sciences, Dalian, Liaoning 116023, P. R. China. E-mail: zhbma@dicp.ac.cn

[c]Hefei National Laboratory for Physical Sciences at the Microscale, CAS Key Laboratory of Strongly-Coupled Quantum Matter Physics, Department of Chemical Physics, University of Science and Technology of China, Hefei, Anhui 230026, P. R. China. E-mail: zengj@ustc.edu.cn

[d]Department of Chemistry, College of Science, Southern University of Science and Technology, Shenzhen, Guangdong 518055, P. R. China.

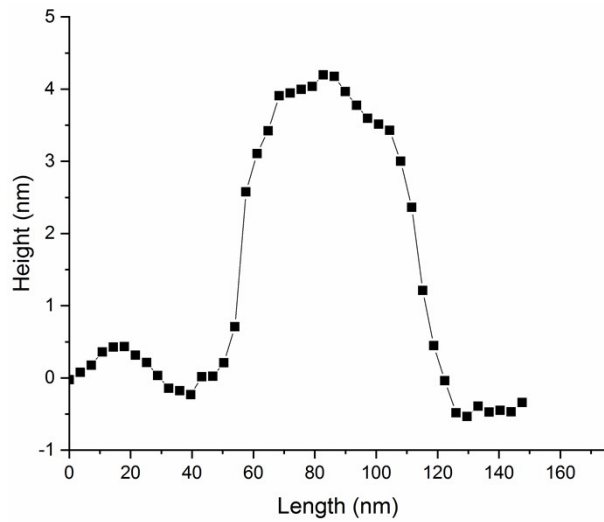[#]These authors contributed equally to this work.

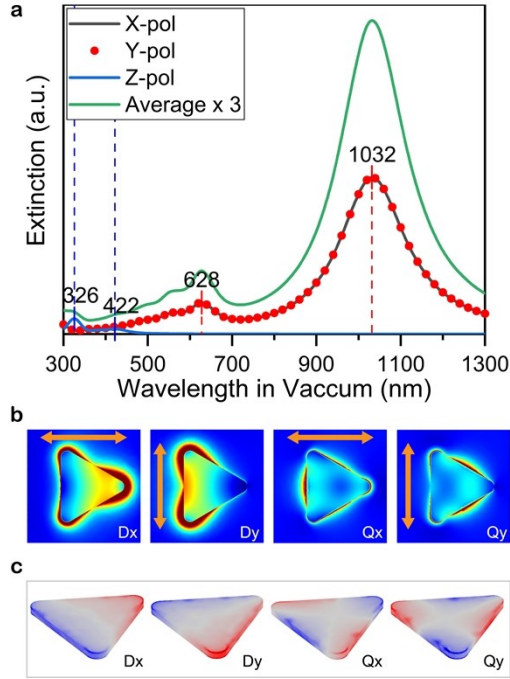**Fig. S1** Data from atomic force microscopy characterization.

Fig. S2 Simulated extinction spectrum, surface charge distribution, and near electric field. (a) Theoretically simulated extinction spectrum of triangular Ag nanoplate in water for different polarizations. X-pol, Y-pol, and Z-pol are for X-polarization, Y-polarization, and Z-polarization, respectively. X-polarization and Y-polarization are parallel to one altitude of triangle and the corresponding side of triangle, respectively. Z-polarization is perpendicular to the top and bottom faces. Total extinction spectrum considering random orientations of nanoplates in solution is calculated as the average of contributions from the three polarizing directions. Polarization-dependent distributions of induced surface charge (b) and near electric field (c) for the in-plane dipole (1032 nm, D_x, D_y) and quadrupole (628 nm, Q_x, Q_y) modes are depicted. The lower-intensity peaks located at 422 nm and 326 nm correspond to the out-of-plane dipole and quadrupole modes, respectively.

Mode analysis of plasmonic eigenmodes (triangular prism on substrate, C_{3V} point group)

The vectorial selection rule by Zhang *et al.* (*Phys. Rev. B* **2010**, *81*, 233407) states that: if the ith component (i=x,y,z) of the electric field $\boldsymbol{E}_n$ of the nth LSPR mode excited by an external field $\boldsymbol{E}_{ext}$, transforms as irreducible representation $\Gamma_{n,i}$ and Γ_{ext}, respectively, the excitation strength of LSPR mode n $\langle E_n | E_{ext} \rangle$ vanishes unless the direct product $\Gamma_{n,i} \otimes \Gamma_{ext}$ contains the totally symmetric irreducible representation A. In the current case, the components of excitation light illuminating the triangular nanoprism, ($E_{ext\ x}$, $E_{ext\ y}$, $E_{ext\ z}$) corresponds to irreducible representions ($\Gamma_{ext\ x}$, $\Gamma_{ext\ y}$, $\Gamma_{ext\ z}$)=(E, E, A_1), as shown in the character table for the C_{3V} point group (Table S1).

Table S1 Character table for the C_{3V} point group.

	E	$2C_3$	$3\sigma_v$	linear, rotations	quadratic
A_1	1	1	1	z	x^2+y^2, z^2
A_2	1	1	-1	R_z	
E	2	-1	0	(x, y) (R_x, R_y)	(x^2-y^2, xy) (xz, yz)

The optical activity of LSPR modes under specific light polarizations are listed below.

Γ_x (dipolar) $\otimes \Gamma_{ext\ x,y}$=$A_1$+$A_2$+E (active)
Γ_x (dipolar) $\otimes \Gamma_{ext\ z}$=E
Γ_y (dipolar) $\otimes \Gamma_{ext\ x,y}$=$A_1$+$A_2$+E (active)
Γ_y (dipolar) $\otimes \Gamma_{ext\ z}$=E
Γ_z (dipolar) $\otimes \Gamma_{ext\ x,y}$=E
Γ_z (dipolar) $\otimes \Gamma_{ext\ z}$=A_1 (active)

$\Gamma_{x2+y2,z2}$ (quadrupolar) $\otimes \Gamma_{ext\ x,y}$=E
$\Gamma_{x2+y2,z2}$ (quadrupolar) $\otimes \Gamma_{ext\ z}$=A_1 (active)
$\Gamma_{(x2-y2,xy)\ (xy,yz)}$ (quadrupolar) $\otimes \Gamma_{ext\ x,y}$=$A_1$+$A_2$+E (active)

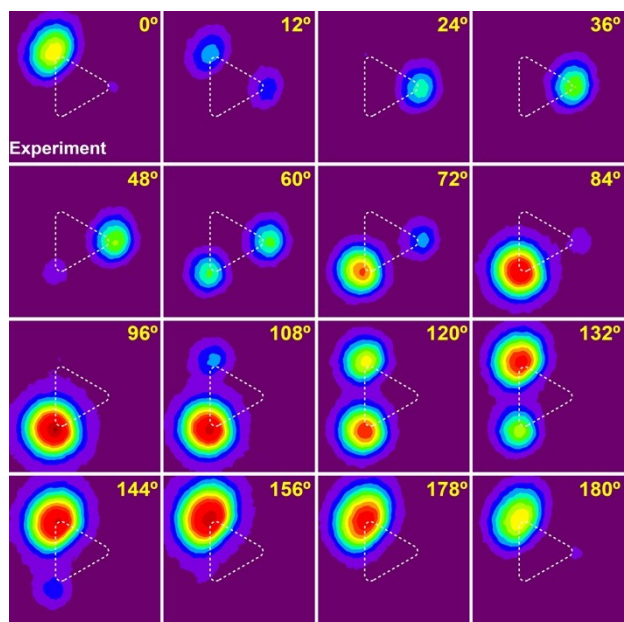$\Gamma_{(x2-y2,xy)\ (xy,yz)}$ (quadrupolar) $\otimes\ \Gamma_{ext\ z}$=E

Fig. S3 Polarization-dependent experimental PEEM images. The raw values for polarization angle were derived from digital readings of half-waveplate. Dash curves are added to show the outline of the triangular nanoplate.
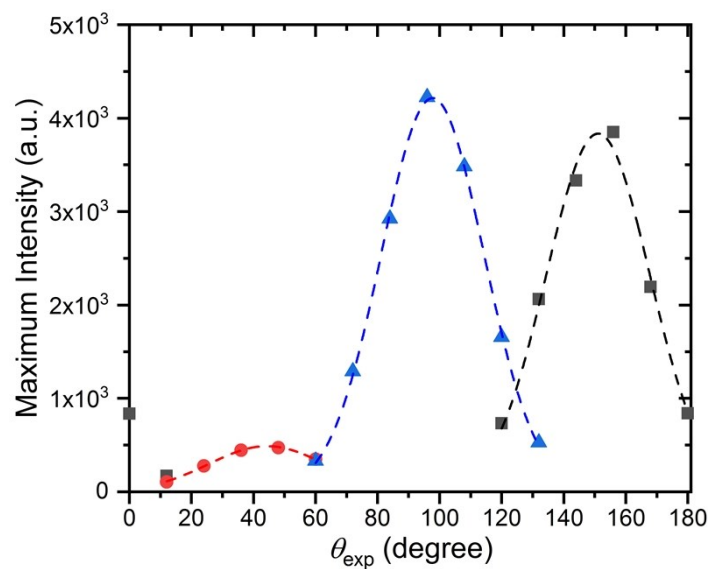
Fig. S4 Maximum intensity of emitted photoelectron. Maximum intensity of emitted photoelectron at three corners of triangle plotted as a function of experimental polarization angles, data from two-dimensional (2D) Gauss function fitting of experimental PEEM images.

Table S2 Comparison of peak positions of photoelectron emission intensity. Comparison of peak positions of photoelectron emission intensity for each bright spot as a function of experimental polarization angle, on the basis of maximum and total intensities obtained by fitting experimental PEEM images with two-dimensional (2D) Gauss function.

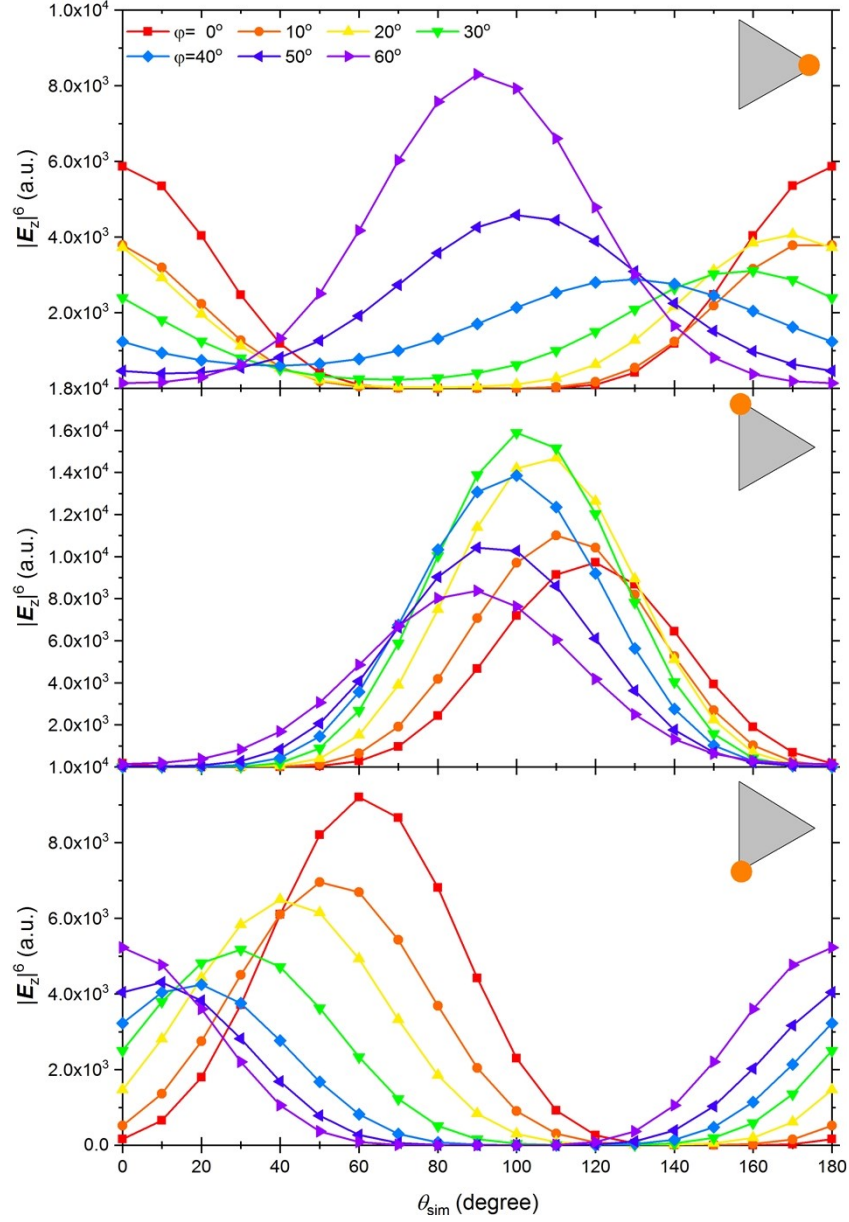| 2D Gauss Fitted by	Peak-1	Peak-2	Peak-3
maximum intensity	44º	98º	151º
total intensity	43º	98º	153º

Fig. S5 Simulated electric field strength with a wide range of azimuth angles. Simulated electric field strength as $|E_z|^6$ at three tips of the top triangular face plotted as a function of theoretical polarization angle, for azimuth angles ranging from 0° to 60° (see the main text for the definition of polarization and azimuth angle used in theoretical modelling).
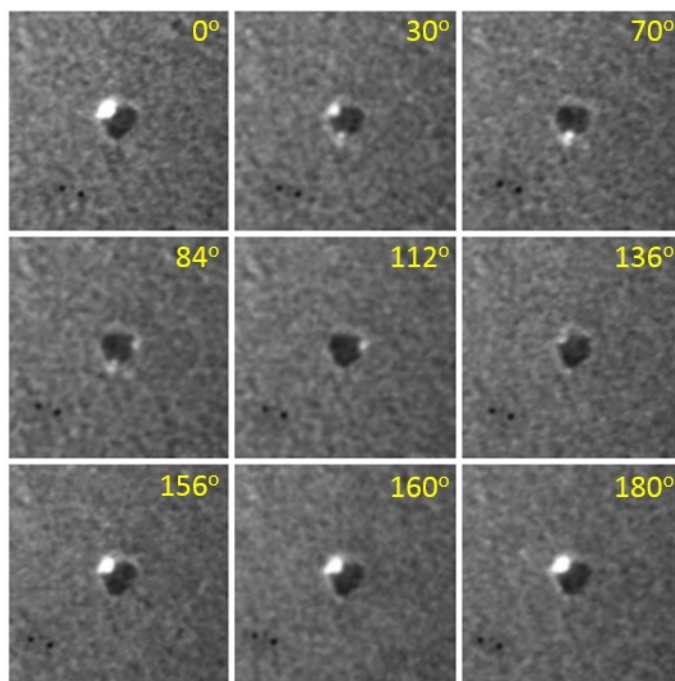
Fig. S6 Polarization-dependent experimental PEEM images. Polarization-dependent experimental PEEM images for one selected nanoparticle, exemplifying pattern with two dark spots and one bright spot for specific spatial orientation.
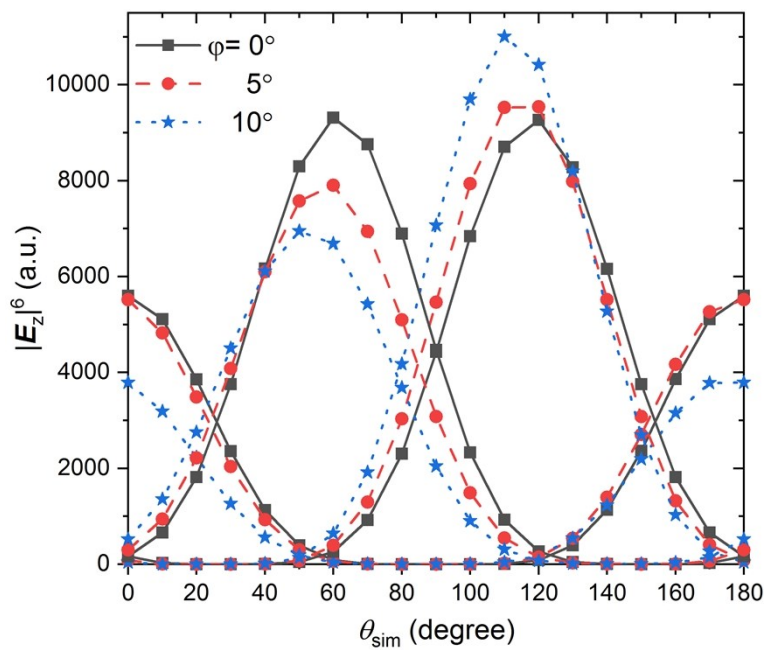
Fig. S7 Simulated electric field strength with small azimuth angles. Simulated electric field strength as $|E_z|^6$ at three tips of the top triangular face plotted as a function of theoretical polarization angle, with azimuth angles of 0°, 5°, and 10°.

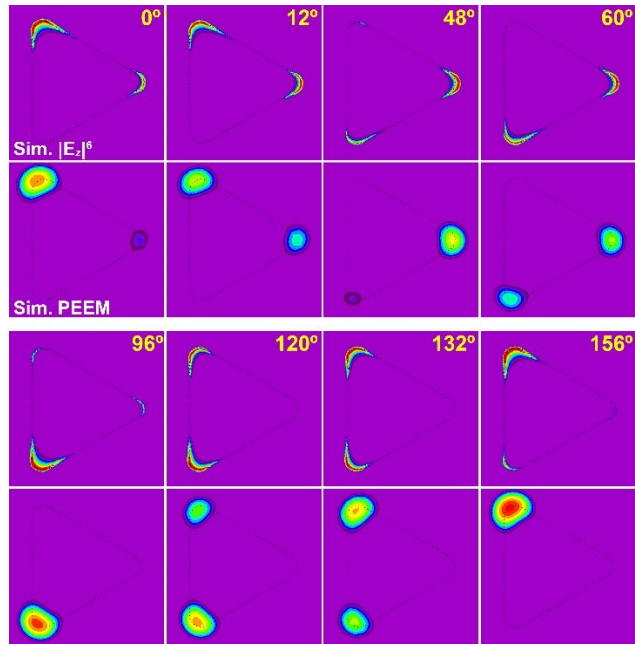**Fig. S8** Simulated electric field strength and PEEM images. Simulated electric field strength as $|E_z|^6$ and PEEM images. Simulated PEEM images are derived by convoluting the electric field using 2D Gaussian profile with a waist of 30 nm.